Headline Articles

Characterization of Ag^+-Exchanged Zeolite A with H_2 and CO Adsorption by FTIR

Ping Wang, Shuwu Yang, Junko N. Kondo, Kazunari Domen,* and Toshihide Baba[1]

Chemical Resources Laboratory, Tokyo Institute of Technology, 4259 Nagatsuta, Midori-ku, Yokohama 226-8503

[1]Chemistry & Material Engineering, Shinshu University, 4-17-1, Wakasato, Nagano 380-8553

Received February 18, 2004; E-mail: kdomen@res.titech.ac.jp

The reversible reduction–oxidation processes of Ag^+ ions in Ag^+-exchanged zeolites A (AgA) with H_2 and O_2 adsorption were studied by Fourier transform infrared (FTIR) spectroscopy. CO adsorption was carried out at low temperature to probe the functional groups present on AgA (before and after H_2 adsorption) and their locations in the channels of zeolite. The hydroxy groups were formed upon H_2 (D_2) adsorption on AgA with different IR frequencies depending on the degree of Ag^+-exchange. It was found that these generated hydroxy groups mainly locate inside the β-cages in AgA at 30%-exchange degree, as evidenced by the inaccessibility of CO due to the small six-oxygen ring windows. On the contrary, the hydroxy groups, which had already been formed before H_2 adsorption due to the dissociation of H_2O on Ag^+ ions, could interact with CO, showing an IR band at 2156 cm^{-1}. This indicates that of hydroxy groups of this type are situated inside the larger α-cages containing 8-membered rings or on the external surface. The CO stretching band of CO–Na^+ adducts appeared at 2165 cm^{-1} and could be easily removed by evacuation, while the CO–Ag^+ species was detected at 2182 cm^{-1} and was highly resistant toward evacuation even at ambient temperature.

Addition of guest cations into the channels and cavities of zeolite can remarkably affect the catalytic activity, selectivity, as well as the adsorptive behavior. Ag^+-exchanged zeolites provide examples of such changes. They have been of great interest because of their potential utilization in light-write and light-erase materials,[1] and in many possible applications as catalysts in several chemical reactions, such as cleavage of water into hydrogen and oxygen,[2] ethanol oxidation to acetaldehyde,[3] isomerization of *n*-butenes,[4] as well as aromatization of alkanes, alkenes, and methanol.[5,6] Ag^+-exchanged zeolites also have been widely studied in various NO_x removal processes.[7,8] Recently, it was found that methane could be easily activated on AgY zeolite at 423 K.[9] In addition, AgA is also a potential photocatalyst for CO conversion to higher carbon compounds, and for reduction of CO_2 using solar energy.[10]

Since Beyer et al.[11] reported on the appearance and disappearance of hydroxy groups upon adsorption of H_2 and O_2 on AgY zeolite, a lot of work have been devoted to investigation of the reduction–oxidation processes of Ag^+-exchanged zeolites.[1] Formation of Ag_n^{m+} ($n > m$) cluster due to the reduction of Ag^+ ion, either by vacuum dehydration at high temperature or by introduction of specific reducing agents such as H_2, is especially attracting much attention and has been studied extensively by various techniques.[1] The locations of the extraframework silver and the formed Ag_n^{m+} ($n > m$) clusters in relation to the aluminosilicate framework are of primary importance for elucidating the effects of silver on the catalytic and adsorptive properties of zeolite. On the other hand, AgA zeolite provides an excellent model system for studying the mechanism for the formation of noble metal clusters within channels and cavities of zeolite, due to its high symmetry and the reversible reduction–oxidation characteristics of silver. However, so far the nature of these silver cationic clusters and locations is still being debated.

It is generally believed that silver clusters formed at high temperatures in AgA zeolite are located inside β-cages. In zeolite A, alumina and silica tetrahedrons are bonded together to form truncated octahedrons, each composed of 24 tetrahedrons denoted as sodalite cavities, or β-cages which constitutes the channel structure of zeolite A. Figure 1 shows the α-cage, β-cage and 4-MR (member ring), 6-MR as well as 8-MR of A-type zeolite. The entrance to β-cage from α-cage is only possible through a six-membered ring, which is called a hexagonal window. The hexagonal window is too small (0.23 nm in diameter) to allow most adsorbates to get into β-cage. The extraframework cations such as Na^+, Ag^+, and H^+, as needed to balance the anionic charge of the zeolite framework, are distributed in different crystallographic sites and can significantly affect its relevant properties. According to earlier X-ray investigations of zeolite NaA, twelve Na^+ ions are distributed in its unit cell as follows.[12] Eight Na^+ ions are placed near the centers of the 6-MRs of the β-cage and occupy all of these windows (Na I sites). Three of the remaining four Na^+ ions are located in 8-MRs of the α-cage (Na II sites), whereas the last Na^+ is found

Published on the web September 10, 2004; DOI 10.1246/bcsj.77.1627

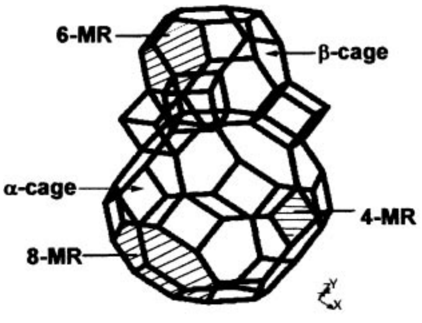

zeolite A

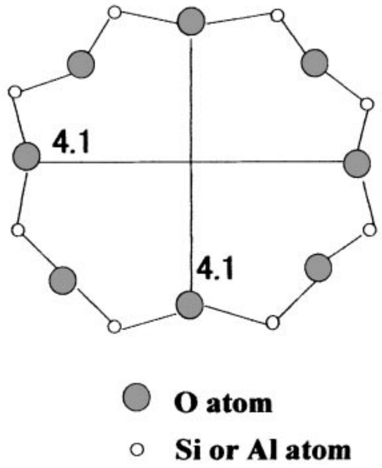

8-MR of zeolite A viewed from <100> direction

Fig. 1. Framework and 8-MR of zeolite A.

near a 4-MR (in α-cage) (Na III sites), which appears to be the least thermodynamically stable because the distance from this Na^+ ion to framework oxygens is the longest, and thus it will be exchanged first by any other type of cation. It has been demonstrated that Ag^+ ions occupy similar positions in the crystal structure to those determined for Na^+ ions.[13]

Although the excellent reactivity of Ag^+-exchanged zeolite is suggested to be related with the redox properties of Ag^+, the active sites responsible for the above-mentioned reactions are still far from being fully understood. This uncertainty arises because several types of functional species, such as Lewis acid sites including isolated silver cations (Ag^+) and silver cationic clusters ($Ag_n{}^{m+}$), Brønsted acid sites with different OH groups, and hydrogenation/dehydrogenation centers (Ag^0) may be involved in these reactions. Additionally, as mentioned above, some debate still exists on the nature and location of the silver cations and silver cationic clusters inside the cavities of AgA with different degrees of Ag^+ exchange.

CO has been used as a probe molecule to detect the state of Ag since it can adsorb on Ag^+ ions by forming stable CO–Ag^+ species through the donation of σ(CO) electron density to the unoccupied 5s orbital of Ag^+, showing IR bands at 2150–2200 cm^{-1} depending on different supports. The metallic Ag does not possess this property, however, because the adsorption of CO on Ag^0 can only form a very weak bond with a predominant π-character at low temperature. An IR band of adsorbed CO on Ag^0 is expected at ca. 2060 cm^{-1} but was rarely observed. Baumann et al.[14] compared the CO adsorption results at room temperature on AgA before and after H_2 adsorption, and assigned the observed IR bands at 2176 and 2153 cm^{-1} to the fast- and slow-CO adsorbing species on Ag^+, respectively, in the case of the unreduced samples. After reduction of AgA with H_2, however, the samples lost their capacity for CO adsorption, depending on the reduction degree. Even so, no reports on CO adsorption on AgA at low temperature are yet available.

Since CO adsorption is favored at low temperature, some carbonyls (such as CO H-bonded to hydroxy groups) that are not stable at ambient temperature can thus be detected. As a result, some very important information on the presence or absence of the hydroxy groups and their Brønsted acidity on the surface of AgA can be obtained. Moreover, adsorption of CO at low temperature can avoid the possible reduction of Ag^+ by CO at room temperature. Therefore, in the present study, we examined the reduction–oxidation processes of Ag^+ ions in AgA zeolites at various degrees of Ag^+ exchange based on H_2 (D_2) and O_2 adsorption spectra obtained by in-situ FTIR spectroscopy. The H_2- or D_2-adsorbed AgA was further examined by CO adsorption at low temperature in order to probe the presence of various functional groups and their locations inside zeolite A.

Experimental

AgA zeolites were prepared from NaA zeolite ($SiO_2/Al_2O_3 = 2.0$, Toso Co. Ltd.) by a conventional ion-exchange method with $AgNO_3$ solution at room temperature, as reported previously.[9] The degrees of Ag^+ exchange examined in this work are 30, 60, and 100%, as determined by atomic absorption analysis;[9] hereafter, these are denoted as AgA-30, AgA-60, and AgA-100. For IR experiments, a self-supporting wafer of AgA (ca. 20 $mg\cdot cm^{-2}$) was placed in the center of a quartz IR cell equipped with NaCl windows, which was connected to a conventional glass vacuum system capable of a final vacuum of ca. 1×10^{-5} Torr (1 Torr = 133.3 Pa). All IR spectra were recorded on a JASCO WS/IR-7300 spectrometer with a mercury–cadmium telluride (MCT) detector. A total of 64 scans were collected at a resolution of 4 cm^{-1} for each spectrum. The samples were pretreated in situ with O_2 at a heating rate of 0.4 $K\cdot min^{-1}$ from room temperature to 673 K, maintained at that temperature for 1 h, and then evacuated for a further 1 h. After pretreatment, the color of the sample changed from gray-white to yellow then to brick-red, indicating the formation of silver cationic clusters. The yellow color was reported to be due to isolated linear $Ag_3{}^{2+}$ clusters, while the brick-red color corresponded to 2–4 interacting $Ag_3{}^{2+}$ clusters inside β-cages.[15]

H_2 (D_2) adsorption (100 Torr) was performed at room temperature after purification by passage through a liquid-nitrogen trap for at least 30 min. CO adsorption was carried out at 150 K after purification using the liquid-nitrogen trap. "H_2- or D_2-adsorbed AgA" refers to AgA samples that were subjected to H_2 or D_2 adsorption at 298 K for 30 min followed by pumping off of gaseous H_2 or D_2 at 298 K for 20 min. All the IR spectra given here are background-subtracted unless otherwise indicated. XRD patterns revealed that the AgA crystalline structure remains unchanged after the H_2/D_2 adsorption under the present conditions.

Results and Discussion

H_2–O_2 Adsorption Cycle on AgA-30. In order to observe the reduction–oxidation properties of AgA, we cycled an H_2–O_2 adsorption on AgA-30. H_2 adsorption was performed at room temperature for 30 min, followed by evacuation at the same temperature to remove the gaseous H_2. For O_2 adsorption, O_2 (120 Torr) was introduced to the system after H_2 adsorption, and then the sample was heated at a heating rate of 0.4 $K\cdot min^{-1}$ from room temperature to 673 K, maintained at that temperature for 1 h, and then evacuated for a further 1 h. The as-observed IR spectra collected at room temperature are shown in Figs. 2A (4000–2800 cm^{-1}) and 2B (950–700 cm^{-1}). Background spectra of AgA (Figs. 2A(b) and 2B(b)) and NaA (Figs. 2A(a) and 2B(a)) are also given for comparison. A broad band at around 3700–3400 cm^{-1}, which has been attributed to the hydrogen-bonded OH stretching vibrations of trace residual water,[16] was observable on each spectrum. The residual water could not be completely removed by evacuation under the present pre-treatment condition. This indicates that the interaction between water and A-type zeolite is very strong. As only 1.5 water molecules per unit cell were reported to be left on the yellow form AgA (dehydrated at 378 K),[17] it can be deduced that residual water in the present AgA pretreated at 673 K is far less than this value. Therefore, effect of the residual H_2O on the subsequent H_2 and CO adsorption is negligible. In the low frequency region, a band at around 785 cm^{-1} was detected only in the spectra of AgA samples (Figs. 2B(b)–(f)); this band is absent in the case of NaA sample (Fig. 2B(a)). This allows us to tentatively attribute this band to the Ag^+-related species. Although its nature is unclear at present, it may correspond to the stretching vibration of the Ag^+–O bond.

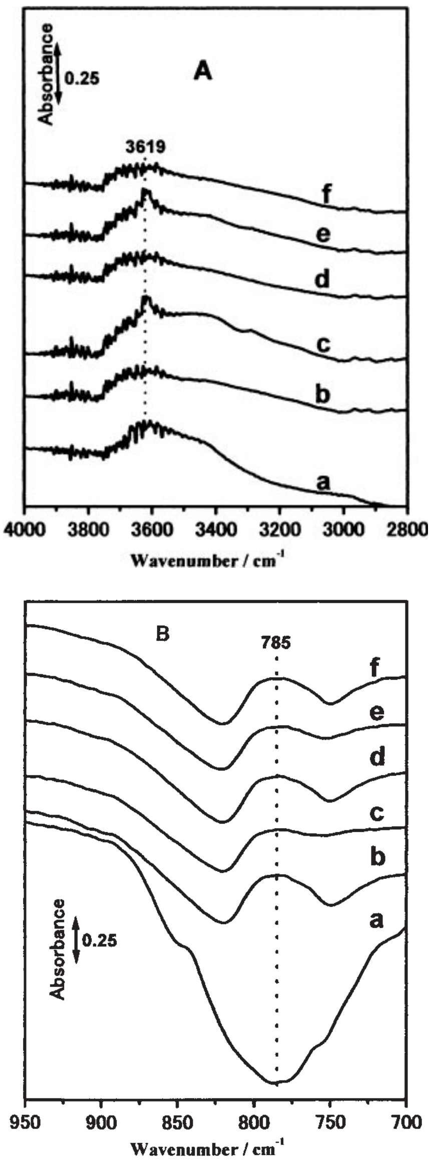

Fig. 2. Background IR spectra of (a) NaA and (b) AgA-30, and the as-observed spectra of H_2 adsorption (298 K, 30 min) and O_2 adsorption (673 K) cycle on AgA-30: (c) first round H_2, (d) first round O_2, (e) second round H_2, and (f) second round O_2. (A) OH stretching region and (B) low frequency region.

Upon adsorption of H_2 on AgA-30 at ambient temperature for 30 min (first round of H_2 adsorption), the formation of bridging OH groups was clearly observed, as evidenced by the appearance of a band at 3619 cm^{-1} (Fig. 2A(c)). Simultaneously, the band at 785 cm^{-1} reduced in intensity to some extent (Fig. 2B(c)). When the sample was re-oxidized with O_2 at 673 K (first round of O_2 adsorption), the band at 3619 cm^{-1} (Fig. 2A(c)) that is attributed to OH groups disappeared (Fig. 2A(d)) with an accompanying restoration in intensity of the band at ca. 785 cm^{-1} (Fig. 2B(d)). If H_2 was re-introduced to the system at 298 K for 30 min (second round of H_2 adsorption) after the first round of O_2 adsorption, similar spectra were obtained to those in Figs. 2A(c) and 2B(c): the sharp 3619-cm^{-1} band emerged (Fig. 2A(e)), accompanied by the weakening in intensity of the 785-cm^{-1} band (Fig. 2B(e)). Furthermore, when the sample was treated with O_2 at 673 K again (second round of O_2 adsorption) after the second round of H_2 adsorption, the same spectra as those after the first round of O_2 adsorption were obtained (Figs. 2A(f) and 2B(f)). These results clearly reflect the reversible reduction–oxidation processes of Ag^+ cations inside the cavities of zeolite, proved by the occurrence and disappearance of the sharp OH band at 3619 cm^{-1} during these H_2–O_2 adsorption cycles. The decrease and recovery in intensity of the 785-cm^{-1} band upon H_2 and O_2 treatment further confirm that this band corresponds to Ag^+-related species.

Comparison of H_2 (D_2) Adsorption on AgA-30, AgA-60, and AgA-100. Adsorption of D_2 on AgA with different degrees of Ag^+-exchange was performed. The background-subtracted spectra of D_2 adsorbed on the AgA-30 sample at 298 K are shown in Fig. 3 (OD stretching and H_2O bending region). Upon introduction of D_2, a new sharp band due to OD stretching vibrations was generated at 2667 cm^{-1} with adsorption time. No bands attributable to D_2O or HDO bending mode were detected at 1700–1400 cm^{-1}, which means that these OD bands are not due to water formation. The frequency ratio of the formed OH to OD band is 1.357 ($3619/2667 = 1.357$), which agrees well with the usually observed isotopic effect of bridging OH groups. Similar results were observed when D_2 was adsorbed on AgA-60 and AgA-100 samples, only dif-

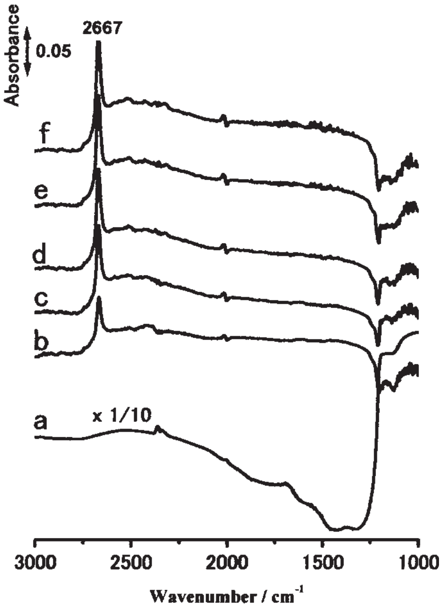

Fig. 3. (a) As-observed background spectrum of AgA-30 and D_2 adsorption (100 Torr) on AgA-30 for (b) 1 min, (c) 5 min, (d) 10 min, (e) 20 min, and (f) 30 min at 298 K.

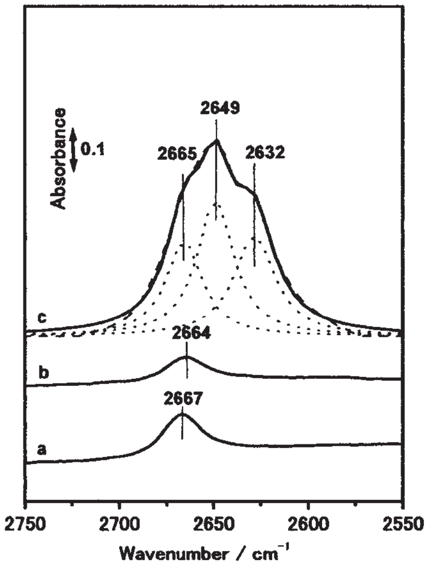

Fig. 4. D_2 adsorption (100 Torr) on (a) AgA-30, (b) AgA-60, and (c) AgA-100 at 298 K for 30 min. (OH stretching region. Dotted lines correspond to deconvoluted spectra, and the dashed line is the fitted spectrum.)

fering in the frequency position and intensity of the OD bands.

A comparison of the IR spectra obtained upon D_2 adsorption over AgA-30, AgA-60, and AgA-100 is reported in Fig. 4 (OD stretching region). The OD bands were observed at 2667 and 2664 cm^{-1} on AgA-30 (Fig. 4(a)) and AgA-60 (Fig. 4(b)), respectively. On the fully Ag^+-exchanged sample, AgA-100, however, a relatively strong OD band was observed, which can be well deconvoluted using the Lorentzian function into three bands at 2665, 2649, and 2632 cm^{-1} (dotted lines on Fig. 4(c)), the dashed line corresponds to the fitted spectrum. Obviously, the OD groups occur at different frequencies depending on the degrees of Ag^+ exchange. The three strong OD bands identified on the AgA-100 sample can be explained in terms of different locations of Ag^+ ions inside the cavity of zeolite. As mentioned in the introduction, the 12 Na^+ ions are distributed in different crystallographic sites in NaA. During Ag^+–Na^+ exchange process, Ag^+ ions first replace the Na^+ ions at the four- (Site III) and the six-oxygen ring (Site I) sites (Ag^+-exchange degree $\leq 75\%$), and then those at the eight-oxygen ring (Site II) sites (Ag^+-exchange degree $> 75\%$).[18] For AgA-30 and AgA-60 samples, the Na^+ ions in Site II are not exchanged by Ag^+ ions. When Ag^+ cations are reduced to Ag^0 atoms upon H_2 or D_2 adsorption, protons replace the Ag^+ ions and become incorporated into the zeolite in order to balance the negative charge of the zeolite framework. Therefore, it is suggested that these OD groups appeared at different positions of IR bands in Fig. 4(c) originate from Ag^+ ions that occupied different crystallographic sites. Correspondingly, the counterpart OD groups are considered to locate on the different sites. However, an unambiguous assignment of these hydroxy groups requires further investigation. Other significant differences, such as adsorption capacity, between the fully and partially exchanged AgA have also been reported.[19]

For NaA zeolite, in contrast, neither OH nor OD bands were detected upon H_2 or D_2 adsorption under the same conditions because of the absence of Ag^+ cations, which serve as the H_2 dissociative adsorption centers. Table 1 summarizes the IR frequencies of OH and OD bands generated in AgA and NaA samples upon H_2 or D_2 adsorption, along with the ν_{OH}/ν_{OD} ratio, which manifests the isotopic effect.

The formation of OD groups upon D_2 adsorption on AgA-100 is pressure-dependent, as shown in Fig. 5. As the D_2 pressure increases, the formation rate of OD groups is accelerated. In the initial adsorption stage (the first 5 min), the OD band increased very fast in intensity, and then began to slow down with prolonged adsorption time whatever the D_2 pressure used.

CO Adsorption on NaA and AgA-30 at Low Temperature. Absorbed CO molecules (via the carbon end of CO adsorption with the cations) provide a convenient spectroscopic probe for the acid sites on the surface of catalysts. Several groups reported CO interaction with Ag^+-exchanged zeolites at ambient temperature.[20–22] The IR frequencies of CO–Ag^+ species were found within the 2200–2150 cm^{-1} spectral region. Recently, CO adsorption on Ag^+/SiO_2 and Ag-ZSM-5 at low temperature was also reported;[22] these results found strong effects of support on the strength of the CO–Ag^+ bond. The carbonyls on Ag^+/SiO_2 are easily decomposed by evacuation even at low temperature. On the contrary, the CO–Ag^+

Table 1. Hydroxy Groups Formed upon H_2 (D_2) Adsorption at 298 K

Sample	OH position /cm^{-1}	OD position /cm^{-1}	ν_{OH}/ν_{OD}
AgA-30	3619	2668	1.356
AgA-60	3613	2664	1.356
AgA-100	3602	2665	1.352
	3591	2649	1.356
	3576	2632	1.359
NaA	Not observed	Not observed	—

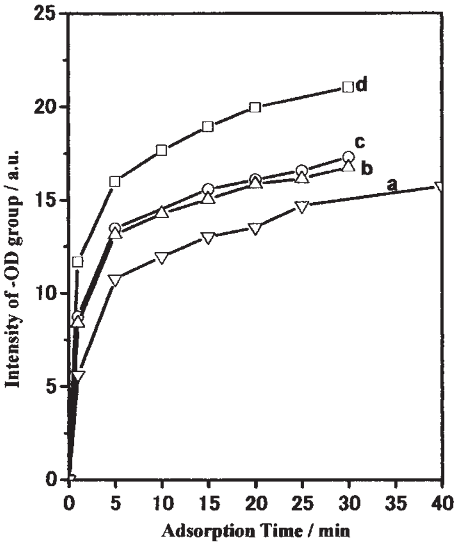

Fig. 5. D_2 adsorption at 298 K on AgA-100 at different pressures. (a) ▽, 5 Torr, (b) △, 40 Torr, (c) ○, 70 Torr, and (d) □, 400 Torr.

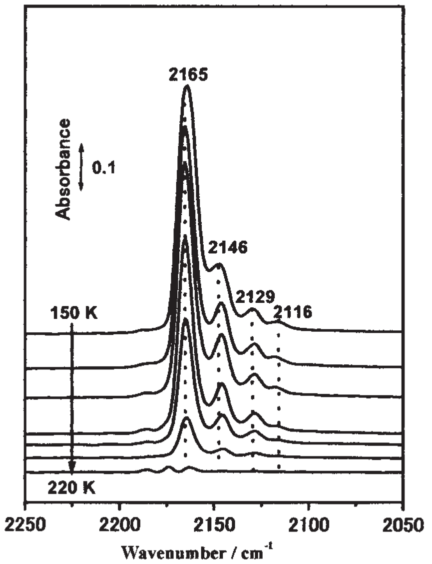

Fig. 6. CO (10 Torr) adsorption on NaA at 150 K followed by gradual warming the IR cell under vacuum.

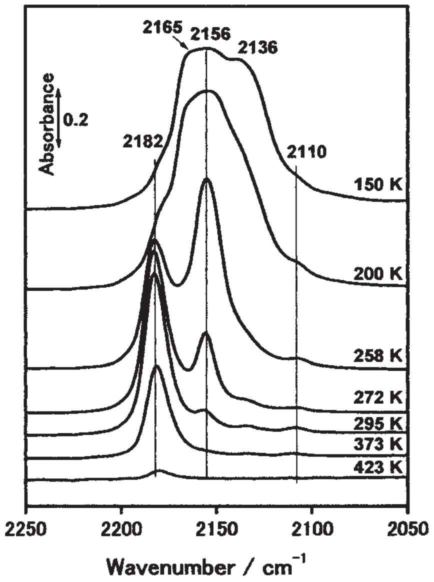

Fig. 7. CO (10 Torr) adsorption on AgA-30 at 150 K followed by gradual warming the IR cell under vacuum.

species formed on Ag-ZSM-5 are highly resistant toward evacuation even at ambient temperature. In order to characterize the different silver hydroxy groups and various cations present on AgA-30 before and after H_2 (D_2) adsorption, we performed CO adsorption at 150 K in the present work.

As a reference, CO adsorption on NaA zeolite was first performed at 150 K and then the IR cell was gradually warmed under vacuum. The CO adsorption on NaA results in four IR bands at 2165, 2146, 2129, and 2116 cm^{-1} at 150 K in the CO stretching region (Fig. 6). The band at 2146 cm^{-1} has been attributed to CO physically trapped inside zeolite channels, and the two bands at 2129 and 2116 cm^{-1} could represent the rotavibrational contribution of quasi-free CO molecules trapped in nanocavities, as suggested by Zecchina et al.[23] The strong band at 2165 cm^{-1}, which was also detected when CO was adsorbed on NaA at room temperature in the presence of gaseous CO (spectrum is not shown), can be assigned to CO linearly adsorbed on Na^+ cations. All of these four bands disappeared in the course of warming the IR cell under vacuum, indicating that the CO–Na^+ species is easily decomposed even at low temperature. Although it is well known that Na^+ ions are distributed in different sites in NaA zeolite, only a single sharp IR band at 2165 cm^{-1} due to the CO–Na^+ species was observed here, which suggests that not all of the Na^+ ions located inside NaA are accessible for CO at low temperature.

After introduction of CO (10 Torr) to the AgA-30 sample (before H_2 adsorption) at 150 K, a set of bands at 2182, 2165, 2156, 2136, and 2110 cm^{-1} emerged in the CO stretching region, as shown in Fig. 7. Gradual warming of the IR cell under vacuum gave rise to successive disappearance of the bands at 2136–2110, 2165, and 2156 cm^{-1}, and finally of the 2182-cm^{-1} band. The band at 2165 cm^{-1} coincides with the IR band position of CO adsorbed on Na^+ ions, and this species can be removed at around 220 K under vacuum. The band at 2156 cm^{-1} gradually weakened with increasing temperature, but remained observable up to room temperature. The two IR bands at 2136 and 2110 cm^{-1} could be related to the rotavibrational contribution of quasi-free CO molecules trapped in nanocavities, as in the case of NaA.

According to Ref. 22, the IR band observed at 2192 cm^{-1} upon CO adsorption on Ag^+-ZSM-5 can be assigned to CO–Ag^+ species. Accordingly, the band at 2182 cm^{-1} in Fig. 7 is attributed to the formation of CO–Ag^+ species. The assignment of this band to CO–Ag^+ species is further supported by the IR results of CO adsorbed on H_2-adsorbed AgA-30 (shown in Fig. 8). Spectra similar to those in Fig. 7 were obtained when CO was adsorbed on H_2-adsorbed AgA-30 sample at 150 K, only differing in the intensity of the band at 2182 cm^{-1}. By comparing IR spectra collected at 272 K when CO was adsorbed on AgA-30 and H_2-adsorbed AgA-30 samples (Fig. 9, CO stretching region), we see that H_2 adsorption has weakened the band at 2182 cm^{-1} in intensity by 95%, while

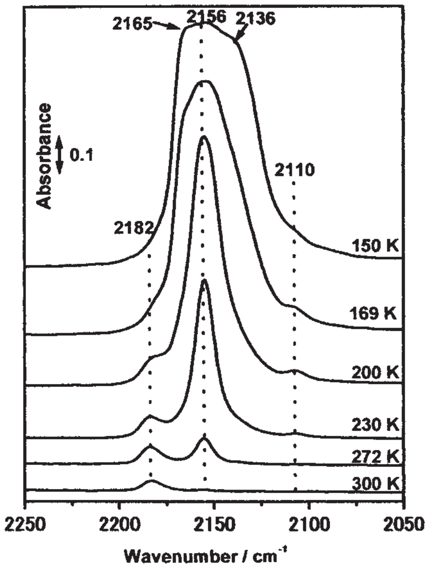

Fig. 8. CO (10 Torr) adsorption on H_2-adsorbed AgA-30 at 150 K followed by gradual warming the IR cell under vacuum.

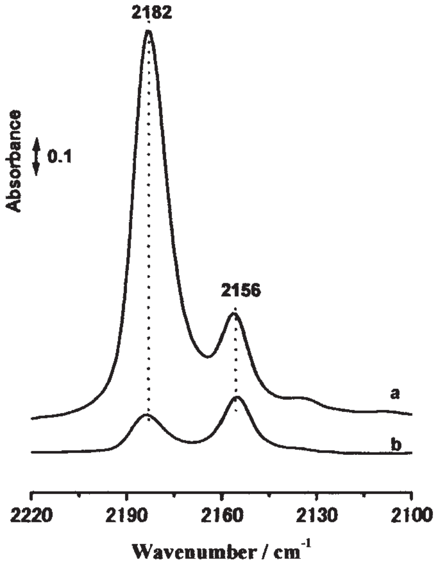

Fig. 9. IR spectra collected at 273 K when CO (10 Torr) was adsorbed on (a) AgA-30 before H_2 adsorption; (b) H_2-adsorbed AgA-30.

the band at 2165 cm^{-1} remained almost unchanged. However, when the sample was re-oxidized with O_2 at 673 K followed by CO adsorption under the same conditions, the intensity of the 2182-cm^{-1} band was recovered completely.

The weakening and recovery of the 2182-cm^{-1} band during the H_2–O_2 adsorption cycle can be attributable to the redox properties of silver cations: Ag^+ was reduced to Ag^0 upon H_2 adsorption on AgA, and Ag^0 was then re-oxidized into Ag^+ when treated with O_2. As mentioned before, an IR band due to CO adsorbed on Ag^0 is expected at ca. 2060 cm^{-1}, but is rarely observed,[24] since adsorption of CO on Ag^0 can form only a very weak bond with a predominant π-character at low temperature. No band related to the formation of CO–Ag^0 species was observed in this work. The CO–Ag^+ species formed on AgA, showing an IR band at 2182 cm^{-1}, is highly resistant toward evacuation even above ambient temperature, indicating a relatively strong σ-bond, with the π-back-donation. This is because, when only a σ-bond is formed between CO and a metal cation, the respective complexes are easily decomposed upon evacuation.[25] However, this is not the case for CO–Ag^+ species formed on AgA sample. In addition, according to a literature report,[26] the extinction coefficient of CO attached to Ag^+ sites (measured for the band at 2170 cm^{-1} observed on Ag_2O/Al_2O_3) is 1.3×10^{20} $cm^2 \cdot mol^{-1}$, which is one order of magnitude lower than that of CO–Cu^+ carbonyls (1.5×10^{21} $cm^2 \cdot mol^{-1}$, band at 2140 cm^{-1} on CuO/Al_2O_3). The extinction coefficient for CO–Ag^+ is, moreover, higher than that measured for typical σ-bond CO species (for example 1.4×10^{19} $cm^2 \cdot mol^{-1}$ for the CO–Ti^{4+} band at 2190 cm^{-1} on TiO_2), which indicates, though weak, some π-back-donation in the CO–Ag^+ species. Theoretical evidence of π-back-donation in the CO bonding to d^{10} metal ion sites was also given.[27,28]

The assignment of the band at 2156 cm^{-1} in Figs. 7 and 8 seems to be more complicated. Hadjiivanov and Knözinger[22] have assigned a similar band to CO H-bonded to surface hydroxy groups when CO was adsorbed on Ag-ZSM-5 at 85 K, since it changed in intensity simultaneously with the shift of a broad OH band at ca. 3200 cm^{-1} to ca. 2800 cm^{-1}. However, Baumann et al.[14] concluded that CO had two types of adsorption kinetics on AgA: fast- and slow-chemisorption. When AgA was exposed to CO at room temperature, an IR band observed at 2174 cm^{-1} was attributed to fast chemisorbed CO–Ag^+ species. After prolonged exposure of AgA to CO, the 2174-cm^{-1} band shifted to 2153 cm^{-1}. Therefore, they assigned the band at 2153 cm^{-1} to slow adsorbed CO–Ag^+ species. Considering that it is very possible that Ag^+ ions could be reduced by CO at room temperature in the case of Ref. 14, we apply the assignment of the presently observed band at 2156 cm^{-1} to the CO H-bonded to hydroxy groups.

To confirm this attribution, we gradually dosed CO to D_2-absorbed AgA-30 at 223 K. Figure 10 shows the correlation of integrated intensities of the band at 2156 cm^{-1} and the OD groups at 2667 cm^{-1} as a function of dosed amount of CO. It revealed that the intensity of band at 2156 cm^{-1} progressively increased with increasing CO dosages, while the band at 2667 cm^{-1} decreased in a mutual-complementing way. This means that the increase of the band at 2156 cm^{-1} is at the cost of consumption of the OD groups. On the other hand, the 2156-cm^{-1} band can be removed by prolonged evacuation at 223 K, which is consistent with the properties of H-bonded species, i.e., the hydrogen bond is weak in nature.

Locations of the CO–Ag^+ Species and the Formed Hydroxy Groups in AgA-30. Considering that a CO molecule is too large (ca. 0.38 nm in diameter[29]) to penetrate into β-cages through the small 6-MR window (0.23 nm in diameter), the presently observed CO–Ag^+ species with the IR band at 2182 cm^{-1} are not likely to be located inside the β-cages. Rather, they would be situated inside the larger α-cages consisting of 8-MR (0.41 nm in diameter as shown in Fig. 1).

Even if the 8-MR of α-cages is larger than the CO molecule, it is not easy for CO to access the Ag^+ ions in α-cages at low

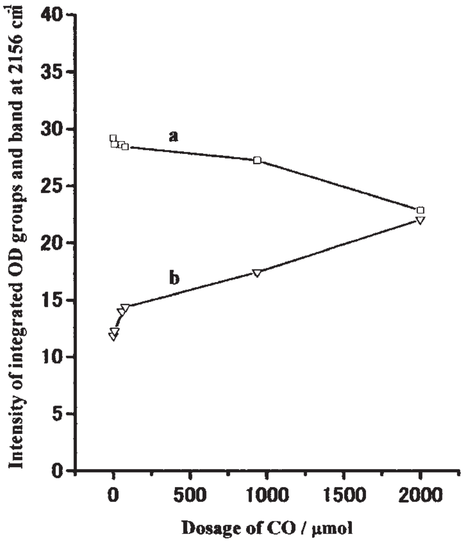

Fig. 10. Integrated intensity of the OD band (2667 cm^{-1}) (a) □, and the 2156-cm^{-1} band (b) ▽, as a function of CO dosing amount on D_2-adsorbed AgA-30.

temperature. As shown in Fig. 7, the band at 2182 cm^{-1} is very weak at 150 K. It first progressively grew in intensity with increasing temperature (up to 295 K), then weakened with further increase in temperature, and finally disappeared at around 423 K. This is caused by the retardation of residual Na^+ ions. When the Ag^+-exchange degree is equal or lower than 75%, the three residual Na^+ ions (Site II) are present near the center of 8-MRs, which would partially block CO from entering the α-cages through the 8-MR at low temperature. In the course of gradual warming of the IR cell to 295 K, this hindrance of Na^+ ions becomes less, due to weakening of the interaction between Na^+ ions and CO as well as an increase in Na^+ mobility and excitation of zeolite lattice vibration. This allows more CO molecules to enter into the α-cages from Na^+ sites, accompanying an increase in intensity of the 2182-cm^{-1} band with temperature. Upon further increasing temperature (above 295 K), the amount of CO absorbed on Ag^+ decreased, and thus the intensity of the band at 2182 cm^{-1} decreased.

Because there is no supply of CO from gas phase, CO–Ag^+ species (2182 cm^{-1}) are formed by conversion of CO appearing at 2156 cm^{-1}, by increase in temperature. It should also be noted that no bands attributable to silver cationic clusters were detected by CO adsorption, indicating that these silver clusters are located in the β-cages, which is consistent with the proposal of Gellens et al. using X-ray powder diffraction method and reflectance spectroscopy.[15]

The locations of the hydroxy groups formed upon H_2 or D_2 adsorption on AgA are also of great interest. Figure 11 compares the OD band of D_2-adsorbed AgA-30 before and after CO adsorption at 150 K. After CO was adsorbed on D_2-adsorbed AgA-30, the intensity of the OD band at 2667 cm^{-1} was slightly decreased. Meanwhile the intensity of the 2156-cm^{-1} band due to H-bonded CO to hydroxy groups on AgA-30 before and after D_2 adsorption remains almost unchanged (Figs. 7–9), which suggests that the additional hydroxy groups generated upon H_2 (D_2) adsorption give little contribution to the intensity of IR band due to absorbed CO at 2156 cm^{-1}.

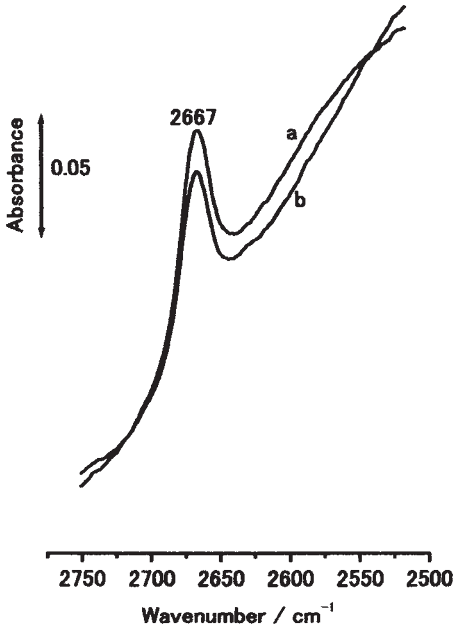

Fig. 11. The OD band at 2667 cm^{-1} of D_2-absorbed AgA (a) before and (b) after CO adsorption at 150 K.

A possible explanation of this phenomenon is the inaccessibility of most of these newly formed hydroxy groups to CO molecules. It can thus be considered that these hydroxy groups produced upon H_2 (D_2) adsorption on AgA-30 are mainly located inside the α-cages, where CO could not reach easily through the small 6-MR windows. In contrast, the hydroxy groups already present on AgA-30 before H_2 (D_2) adsorption may be located on the external surface or inside α-cages in zeolite A.

These results provide evidence that some amount of hydroxy groups, which were difficult to directly observe from their background IR spectra, exist on the dehydrated AgA samples. These hydroxy groups could be due to the dissociation of water molecules on Ag^+ ions during pretreatment at high temperature because no such bands were detected on NaA directly or indirectly by CO adsorption.

CO Adsorption on AgA-60 and AgA-100 at Low Temperature. The spectra of CO adsorbed on AgA-60 (Fig. 12) at 150 K were very similar to those of CO adsorbed on AgA-30. All the bands can be assigned in the same way as discussed above in the case of AgA-30. But as more Ag^+ ions are present on AgA-60, the band at 2184 cm^{-1} due to CO–Ag^+ became broader. However, for AgA-100, the spectra as shown in Fig. 13 are quite different. A very strong and broad band was observed at 150 K. It contains several bands, but they could not be distinguished from each other. Due to the absence of Na^+ ions on the 8-MRs at 100% Ag^+-exchange degree, the observed Ag^+–CO species is relatively strong even at low temperature and is centered at 2184 cm^{-1}. With increasing temperature, this broad band gradually narrowed until it disappeared at around 500 K. A further investigation is needed to confirm the existence of $Ag_n{}^{m+}$–CO as well as formation of CO–Ag^+ species at different sites.

Conclusion

In summary, upon H_2 or D_2 adsorption on AgA at room

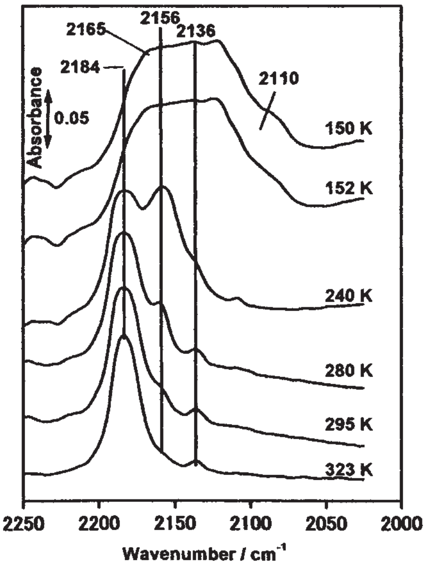

Fig. 12. CO (10 Torr) adsorption on AgA-60 at 150 K followed by gradual warming the IR cell under vacuum.

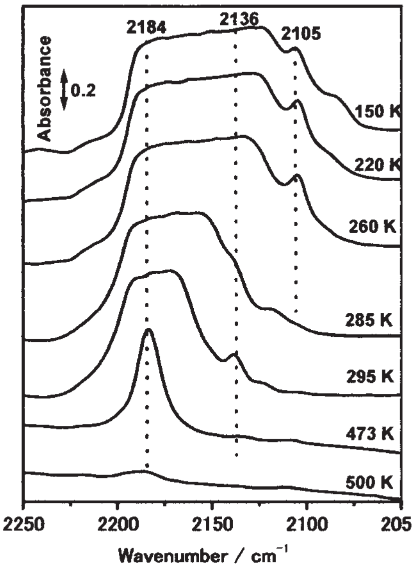

Fig. 13. CO (10 Torr) adsorption on AgA-100 at 150 K followed by gradual warming the IR cell under vacuum.

temperature, some hydroxy groups are generated. These hydroxy groups showed different IR frequencies depending on the degrees of Ag^+-exchange and are suggested to originate from different locations of Ag^+ ions inside zeolite A channels. At 30% Ag^+-exchange degree, it was found that the formed hydroxy groups with H_2 or D_2 adsorption were mainly located inside the β-cages, as evidenced by the inaccessibility of CO due to the small 6-MR windows; the other hydroxy groups produced due to dissociation of H_2O on Ag^+ cations can interact with CO (2156 cm^{-1}), indicating that they are situated inside the larger α-cages or on the external surface. At fully Ag^+-exchange degree, quite different behavior was revealed from that at lower Ag^+-exchange degree by the H_2 and CO adsorption.

References

1 T. Sun and K. Seff, *Chem. Rev.*, **94**, 857 (1994).

2 P. A. Jacobs, J. B. Uytterhoeven, and H. K. Beyer, *J. Chem. Soc., Chem. Commun.*, **1977**, 128.

3 D. Lai, J. Li, P. Huang, and D. Wang, *J. Mater. Gas Chem.*, **3**, 211 (1994).

4 H. Förster and R. Seelemann, *J. Chem. Soc., Faraday Trans. 1*, **74**, 1435 (1978).

5 Y. Ono, K. Osako, G.-J. Kim, and Y. Inoue, *Stud. Surf. Sci. Catal.*, **84**, 1773 (1994).

6 Y. Inoue, K. Nakashiro, and Y. Ono, *Microporous Mater.*, **4**, 379 (1995).

7 M. Matsuoka, E. Matsuda, K. Tsuji, H. Yamashita, and M. Anpo, *J. Mol. Catal.*, **107**, 399 (1996).

8 S. Sato, Y. Yu-u, K. Yahiro, N. Mizuno, and M. Iwamoto, *Appl. Catal.*, **70**, L1 (1991).

9 T. Baba, N. Komatsu, H. Sawada, Y. Yamaguchi, T. Takahashi, H. Sugisawa, and Y. Ono, *Langmuir*, **15**, 7894 (1999); T. Baba, Y. Johjo, T. Takahashi, H. Sawada, and Y. Ono, *Catal. Today*, **66**, 81 (2001).

10 R. Beer, G. Calzaferri, J. Li, and B. Waldeck, *Coord. Chem. Rev.*, **111**, 193 (1991).

11 H. Beyer, P. A. Jacobs, and J. B. Uytterhoeven, *J. Chem. Soc., Faraday Trans. 1*, **72**, 674 (1976).

12 D. W. Breck, "Zeolite Molecular Sieves," Wiley, New York (1974), p. 88.

13 J. J. P. M. De Kanter, I. E. Maxwell, and P. J. Trotter, *J. Chem. Soc., Chem. Commun.*, **1972**, 733.

14 J. Baumamm, R. Beer, and B. Waldeck, *J. Phys. Chem.*, **93**, 2292 (1989).

15 L. R. Gellens, W. J. Mortier, and J. B. Uytterhoeven, *Zeolites*, **1**, 11 (1981).

16 J. Howard and J. M. Nicol, *J. Chem. Soc., Faraday Trans.*, **86**, 205 (1990).

17 L. R. Gellens, W. J. Mortier, R. A. Schoonheydt, and J. B. Uytterhoeven, *J. Phys. Chem.*, **85**, 2783 (1981).

18 M. Nitta, S. Matsumoto, and K. Aomura, *J. Catal.*, **35**, 317 (1974).

19 J. Sebastian and R. V. Jasra, *Chem. Commun.*, **2003**, 268.

20 Y. Y. Huang, *J. Catal.*, **32**, 482 (1974).

21 T. Baba, N. Akinaka, M. Nomura, and Y. Ono, *J. Chem. Soc., Chem. Commun.*, **1992**, 339.

22 K. Hadjiivanov and H. Knözinger, *J. Phys. Chem. B*, **102**, 10936 (1998).

23 A. Zecchina, S. Bordiga, C. Lamberti, G. Spoto, L. Carnelli, and C. Otero-Arean, *J. Phys. Chem.*, **98**, 9577 (1994).

24 X. D. Wang and R. D. Greeneer, *Surf. Sci.*, **226**, L51 (1990).

25 G. Busca, *Catal. Today*, **41**, 191 (1998).

26 A. Davydov, "IR Spectroscopy Applied to Surface Chemistry of Oxides," Nauka, Novosibirsk (1984).

27 E. I. Salomon, P. M. Jones, and J. A. May, *Chem. Rev.*, **93**, 2623 (1993).

28 M. F. Garcia, J. C. Conesa, and F. Illas, *Surf. Sci.*, **349**, 207 (1996).

29 J. H. C. Van Hooff and J. W. Roelofsen, *Stud. Surf. Sci. Catal.*, **58**, 241 (1991).